



저작자표시-비영리-변경금지 2.0 대한민국

이용자는 아래의 조건을 따르는 경우에 한하여 자유롭게

- 이 저작물을 복제, 배포, 전송, 전시, 공연 및 방송할 수 있습니다.

다음과 같은 조건을 따라야 합니다:



저작자표시. 귀하는 원저작자를 표시하여야 합니다.



비영리. 귀하는 이 저작물을 영리 목적으로 이용할 수 없습니다.



변경금지. 귀하는 이 저작물을 개작, 변형 또는 가공할 수 없습니다.

- 귀하는, 이 저작물의 재이용이나 배포의 경우, 이 저작물에 적용된 이용허락조건을 명확하게 나타내어야 합니다.
- 저작권자로부터 별도의 허가를 받으면 이러한 조건들은 적용되지 않습니다.

저작권법에 따른 이용자의 권리는 위의 내용에 의하여 영향을 받지 않습니다.

이것은 [이용허락규약\(Legal Code\)](#)을 이해하기 쉽게 요약한 것입니다.

[Disclaimer](#)

Thesis for the Degree of Master of Engineering

Laser-assisted endoscopic submucosal dissection for early gastric cancer

by

Hanjae Pyo

Department of Industry 4.0 Convergence Bionics Engineering

The Graduate School

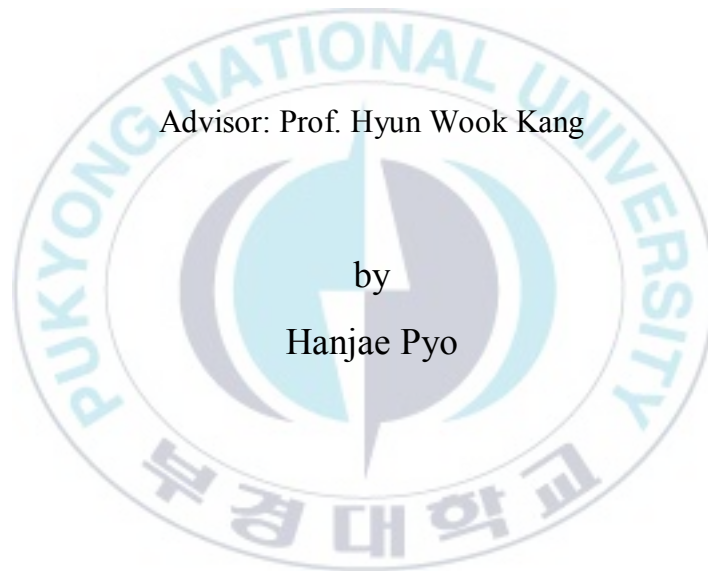
Pukyong National University

February 2021

Laser-assisted endoscopic submucosal dissection for early gastric cancer

조기위암 치료를 위한 레이저 응용

내시경 점막하 박리술 연구



Advisor: Prof. Hyun Wook Kang

by

Hanjae Pyo

A thesis submitted in partial fulfillment of the requirements
for the degree of

Master of Engineering

in Industry 4.0 Convergence Bionics Engineering,
The Graduate School, Pukyong National University

February 2021

Laser-assisted endoscopic submucosal dissection for early gastric cancer

A dissertation

by

Hanjae Pyo

Approved by:

(Chairman) Sang-Hyug Park Ph. D

(Member) Myunggi Yi Ph. D

(Member) Hyun Wook Kang Ph. D

February 19, 2021

Laser-assisted endoscopic submucosal dissection for early gastric cancer

Hanjae Pyo

Department of Industry 4.0 Convergence Bionics Engineering, The Graduate School

Pukyong National University

Abstract

내시경 점막하 박리술 (endoscopic submucosal dissection)은 림프전이의 가능성이 없는 조기 위암에 대하여 국소적으로 병변 부위만을 절제하여 박리시키는 보존적 치료 방법이다. 내시경 점막하 박리술은 위암 병변의 크기와 관계없이 일괄 절제가 가능하다는 장점이 있고 병변의 완전 절제율이 높아서 임상적으로 좋은 예후가 보고되고 있다. 하지만 내시경 점막하 박리술의 높은 수술 난이도와 천공 및 출혈이라는 한계 때문에 이를 개선하기 위해 다양한 레이저를 사용한 위 점막 절제술이 연구되고 있다. 레이저 점막 절제 시 발생하는 열 반응 및 조직학적 변화에 대한 연구가 지속적으로 보고되고 있지만, 선택적 병변 절제를 위한 최적의 레이저 조건에 대한 연구는 부족한 실정이다. 본 연구에서는 홀뮴 야그 (holmium:YAG) 레이저를 사용한 위 점막 절제의 효과성과 이에 따른 열 반응을 조사하였다. 생체 외 실험에서 정의된

레이저 조건에 의해 위 점막이 완전히 절제되는 것을 확인하였고, 식염수를 점막하층에 주입하였을 때 천공이 발생하지 않고 점막층만 선택적으로 절제할 수 있음을 확인하였다. 또한, 레이저 조사에 의해 발생한 절제 부위 주변의 열변성 현상을 정량적으로 측정하여 내시경 점막하 박리술에 대한 레이저의 임상적 사용 가능성을 평가하였다. 결과적으로 홀몸 야그 레이저는 위 점막을 효과적으로 절제할 수 있고 기존 치료법의 한계점을 개선할 가능성이 있다. 이와 관련하여 기존의 전기소작술과 비교하여 안전성 및 효과성을 평가하는 생체 내 실험 및 임상적 연구가 이루어져야 할 것으로 사료된다.



Table of contents

| | |
|--|------------|
| Abstract | i |
| Table of contents | iii |
| List of figures | vi |
| 1. Introduction | 1 |
| 1.1. Endoscopic submucosal dissection | 1 |
| 1.2. Overview of Ho:YAG laser | 6 |
| 2. Ho:YAG laser treatment in static condition for tissue ablation | 8 |
| 2.1. Purpose | 8 |
| 2.2. Materials and methods | 9 |
| 2.2.1. Procurement of stomach tissue | 9 |
| 2.2.2. Physical parameters of Ho:YAG laser | 9 |

| | |
|---|----|
| 2.2.3. Characterization of photothermal responses ----- | 12 |
| 2.2.4. Histological analysis ----- | 13 |
| 2.3. Results ----- | 15 |
| 2.3.1. Examination of thermal response in stomach tissue ----- | 15 |
| 2.3.2. Evaluation of thermal response in stomach tissue ----- | 18 |
| 2.3.3. Histological evaluation ----- | 20 |
| 3. Translational laser treatment for mucosal incision ----- | 22 |
| 3.1. Purpose ----- | 22 |
| 3.2. Materials and methods ----- | 23 |
| 3.2.1. Experimental set-up for laser treatment ----- | 23 |
| 3.2.2. Laser irradiation on no saline-injected stomach tissue ----- | 26 |
| 3.2.3. Laser irradiation on saline-injected stomach tissue ----- | 26 |

| | |
|---|----------------|
| 3.2.4. Evaluation of laser-ablated stomach tissue | -----27 |
| 3.2.5. Histological analysis | -----28 |
| 3.3. Results | -----29 |
| 3.3.1. Evaluation of Ho:YAG-assisted ESD under no saline injection | -----29 |
| 3.3.2. Evaluation of Ho:YAG-assisted ESD under saline injection | -----33 |
| 3.3.3. Characterization of Ho:YAG-assisted ESD in circular pattern | -----38 |
| 4. Discussion | -----41 |
| 5. Summary | -----47 |
| 6. References | -----48 |
| Acknowledgements | -----52 |

List of figures

- Figure 1.** Standard steps of ESD to remove early gastric cancer (Memorial Sloan Kettering Cancer Center) -----4
- Figure 2.** Various types of endoscopic knives to facilitate cutting performance. (A) IT knife, (B) The second-generation IT knife, (C) Hook knife, (D) Flex knife, and (E) Triangletip knife. (Alberto Larghi and Irving Waxman. 2007) -----5
- Figure 3.** (a) Schematic diagram of experimental set-up for tissue ablation by using optical fiber (M: mucosal layer, SM: submucosal layer, and MP: Muscular propria) and (b) top-view image of laser-treated stomach sample. -----11
- Figure 4.** Evaluation of ablation depth and thermal damage in cross-sectional image of laser-ablated stomach tissue: (a) no laser-treated stomach sample (M: mucosal layer, SM: submucosal layer, and MP: muscular propria), (b) definition of ablation depth (a distance from tissue surface to bottom of ablated groove) and (c) thermal damage (an average value of ①~⑤). -----14

Figure 5. Observation of physical deformation in cross-sectional view of laser-treated stomach tissue: (a) comparison of thermal response of stomach tissue by multiple times of laser pulses and (b) ablation grooves in stomach tissue under various number of pulses irradiation (#21~#30). -----17

Figure 6. Characterization of thermal response in terms of various number of laser pulses (#21~#30): normalization of (a) ablation depth and (b) thermal damage in laser-treated stomach tissue. -----19

Figure 7. Comparison of laser-ablated stomach tissue in cross-sectional images and histology images under various pulse energies: (a) control, (b) 10 pulses (#10), (c) 20 pulses (#20), and (d) 30 pulses (#30) of Ho:YAG laser irradiations. Black arrows represent ablative regions (M: mucosal layer, SM: submucosal layer, and MP: muscular propria). -----21

Figure 8. Experimental set-ups for Ho:YAG-assisted ESD on porcine stomach tissue: (a) schematic diagram of lens systems to obtain 1-mm beam diameter on

tissue surface, (b) translational stage to attain straight ablation pattern, and (c) rotational stage to achieve circular ablation pattern to emulate clinical ESD (OF: optical fiber, PCL: plano-convex lens, BCL: bi-convex lens, M: mucosal layer, SM: submucosal layer, and MP: muscular propria). -----25

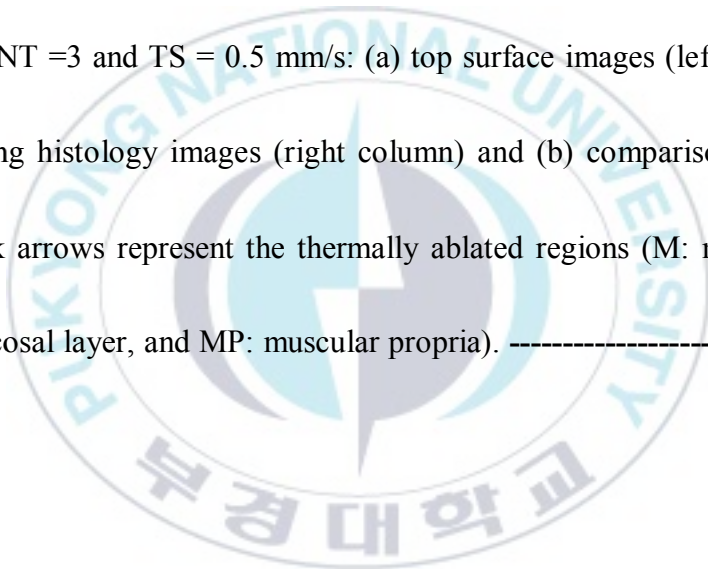
Figure 9. Laser-assisted ESD on ex vivo porcine stomach tissue without saline injection under various surgical parameters: (a) top view images and (b) cross-sectional images of laser-ablated stomach. -----31

Figure 10. Quantification of thermal response of stomach tissue without saline injection under defined treatment conditions: normalization of (a) ablation depths and (b) extent of irreversible thermal injury. -----32

Figure 11. Laser-assisted ESD on ex vivo porcine stomach tissue with saline injection under various surgical parameters: (a) top view images and (b) cross-sectional images of laser-ablated stomach. -----35

Figure 12. Quantification of thermal response of stomach tissue with saline injection under defined treatment conditions: normalization of (a) ablation depths and (b) extent of irreversible thermal injury. -----36

Figure 13. Comparison of circularly-ablated tissue lesion without and with saline injection at NT =3 and TS = 0.5 mm/s: (a) top surface images (left column) and corresponding histology images (right column) and (b) comparison of ablation depth. Black arrows represent the thermally ablated regions (M: mucosal layer, SM: submucosal layer, and MP: muscular propria). -----40



1. Introduction

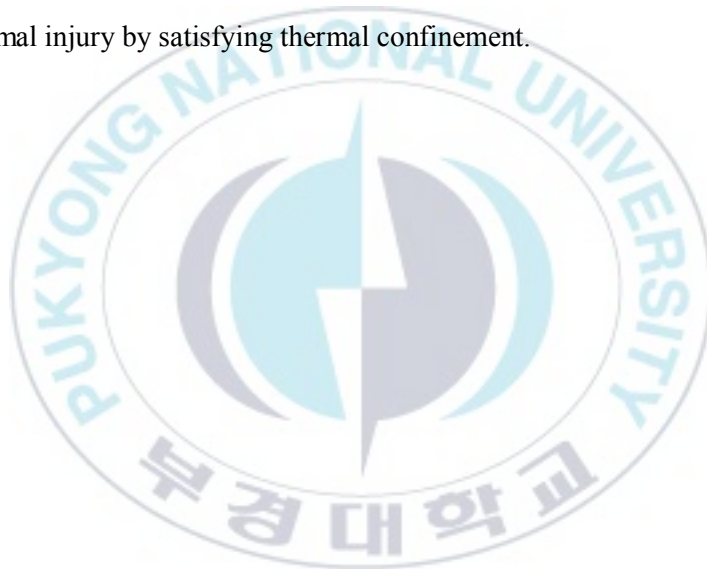
1.1. Endoscopic submucosal dissection

Endoscopic submucosal dissection (ESD) is a stomach-preserving method to remove an early gastric cancer (EGC) without risk of lymphatic metastasis from human stomach [1].

Due to prevalence of cancer screening program, detection of EGC have been increased and ESD have been preferable technique for EGC. ESD is composed with several steps: 1) marking a target lesion to be incised, 2) injecting functional fluid into a submucosal layer to lift a mucosal layer from muscular propria, 3) cutting circumferential tissue of the lesion, and 4) dissecting the bottom of the lesion to en bloc remove the abnormal tissue from the stomach [2-4]. Several studies have demonstrated the outstanding performance of ESD in terms of high resection rate and reduced recurrence [5, 6]. Furthermore, ESD has no particular delimitation of lesion size [7]. However, the potential risks of intraoperative bleeding and perforation on the gastrointestinal tract still remain with possible complications by ESD [5, 8-10]. In addition to, long operation time, difficulty of surgery,

and durability of lifting by injected liquid are quite problematic [11]. Although various types of electrosurgical unit have been suggested to facilitate surgical procedure, the cutting performance is still hard to control during surgery [12, 13]. Because the depth of dissection by ESU is entirely dependent on the handling of an operator, it is often time-consuming to avoid over-cutting the unwanted area that could cause perforation. Recently, technical efforts were reported to employ a laser system as one of alternative surgical tools for ESD. For instance, CO₂ (10.6 μm) and thulium (2 μm) laser systems have been tested for laser-assisted ESD because of high light absorption characteristics (absorption coefficient = 630 cm⁻¹ and 65 cm⁻¹ for CO₂ and thulium, respectively). A study reported that CO₂ laser was examined with ex vivo and in vivo porcine stomach to incise tissue by using a hollow wave guide to deliver light endoscopically. In spite of precise tissue incision, the CO₂ laser still suffered from high transmission loss and tissue carbonization, leading to inefficient ESD outcomes. Another study demonstrated that the thulium laser with high power (~100 W) was able to incise and vaporize soft tissue, including prostate, kidney, and stomach [15]. In fact, a clinical study applied continuous-wave (CW) thulium light to

remove epithelial neoplasm [13,16]. However, the CW irradiation caused significant thermal damage to the surrounding tissue and carbonization at the fiber tip and on the mucosal tissue as a result of excessive heat accumulation. Thus, more effective laser system is still needed to locally ablate both mucosal and submucosal tissue with no or minimal thermal injury by satisfying thermal confinement.



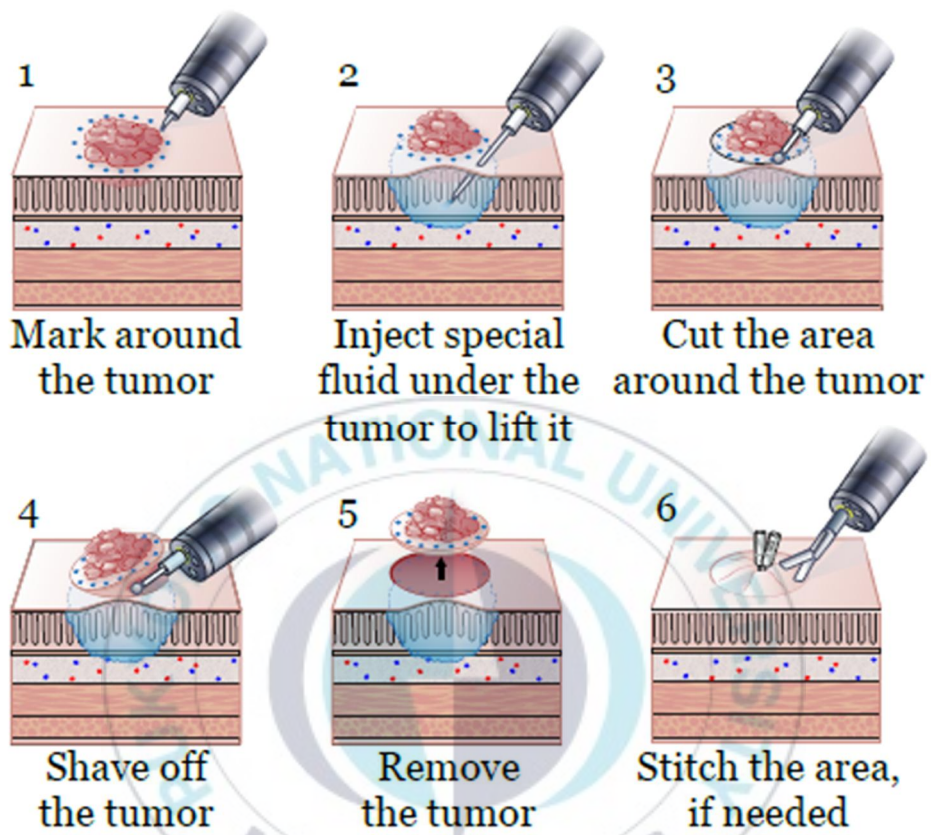


[Figure adopted from (Memorial Sloan Kettering Cancer Center, About Your Endoscopic Submucosal Dissection (ESD) with and Upper Endoscopy. www.mskcc.org)]

Figure 1. Standard steps of ESD to remove early gastric cancer.

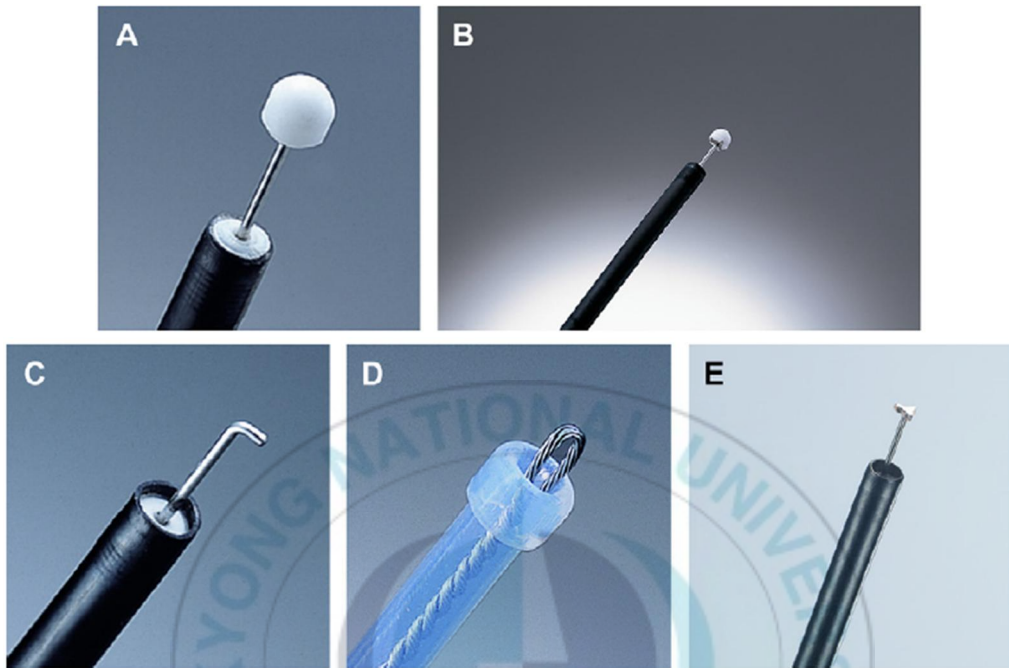


[Figure adopted from (Larghi A, Waxman I (2007) State of the art on endoscopic mucosal resection and endoscopic submucosal dissection. *Gastrointestinal endoscopy clinics of North America* 17 (3):441-469)]

Figure 2. Various types of endoscopic knives to facilitate cutting performance. (A) IT knife, (B) The second-generation IT knife, (C) Hook knife, (D) Flex knife, and (E) Triangletip knife.

1.2. Overview of Ho:YAG laser

Ho:YAG laser is one of medical laser emitting an infrared wavelength of 2.1 μm . Because of strong light absorption by water (absorption coefficient = 30 cm^{-1}), pulsed Ho:YAG laser is applied in tissue ablation such as bladder carcinoma, prostatic hypertrophy, and urethra stricture [14-17]. Under a typical pulse duration of Ho:YAG laser (200~400 μs), thermal effect induced by incident light energy can be confined within a thin layer of soft tissue (~0.4 mm) with minimal heat diffusion. As the volumetric deposition of optical energy and efficient conversion to thermal energy, Ho:YAG laser can induce controlled tissue removal with minimal thermal injury to surrounding tissue. In fact, one research clinically tested Ho:YAG laser (pulse frequency = 15Hz and pulse energy = 1 J) to remove early gastric cancer from patient through ESD procedure [18]. Even if the study demonstrated fine clinical results of Ho:YAG-assisted ESD, scientific investigation about physical responses of gastric tissue during laser irradiation is deficient. Therefore, further studies are still needed to characterize photothermal responses of gastric tissue for effective laser-assisted ESD by using Ho:YAG laser with various physical parameters.

The aim of current study was to verify a therapeutic capacity of Ho:YAG laser to implement ESD under various treatment conditions. The pulsed Ho:YAG laser was employed to ablate *ex vivo* stomach tissue in static and translational environment for incision of mucosal layer.



2. Ho:YAG laser treatment in static condition for tissue ablation

2.1. Purpose

The purpose of this study was to investigate photothermal response of *ex vivo* stomach tissue in static condition for complete elimination of mucosal layer and submucosal layer by using pulsed Ho:YAG laser. It was hypothesized that pulsed Ho:YAG laser can induce volumetric thermal ablation in the porcine stomach tissue. Various laser conditions were employed in Ho:YAG laser system on fixed beam spot in order to remove targeted lesions. After the laser treatment, the ablation depth and the extent of thermal damage were evaluated in quantitative manner.

2.2. Materials and methods

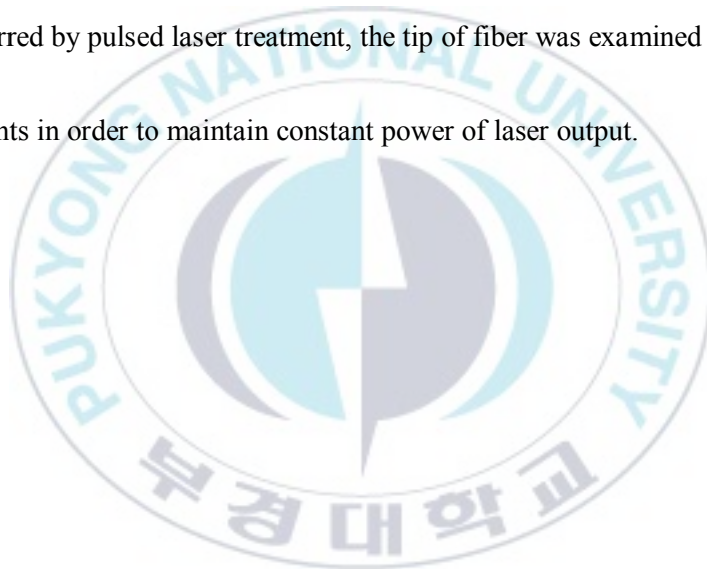
2.2.1. Procurement of stomach tissue

A porcine stomach tissue was procured from a local slaughter house for *ex vivo* experiments. Harvested organ was immediately preserved at - 10 °C in order to prevent dehydration and decomposition. Prior to the experiment, the prepared stomach samples were thawed at room temperature and the tissue consisted of mucosa (~ 2 mm thick), submucosa (~0.5 mm thick), and muscular propria (~1.5 mm thick).

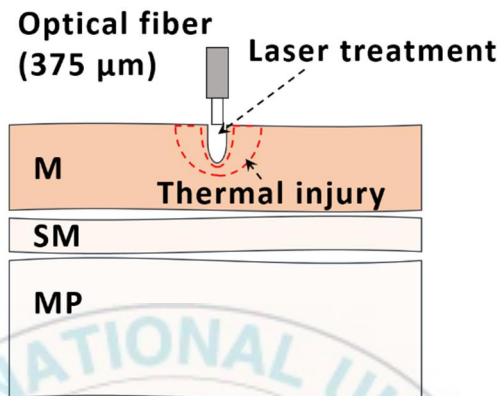
2.2.2. Physical parameters of Ho:YAG laser

A pulsed Ho:YAG laser system ($\lambda = 2.1 \mu\text{m}$ and pulse duration = ~350 μs ; StoneLight™, AMS, San Jose, CA, USA) was employed to ablate the prepared stomach samples. A silica optical fiber (core = 375 μm) was coupled to the laser system to deliver a pulse energy of 1 J at 10 Hz of laser frequency). A photodiode sensor (FL250A-LP2-35, OPHIR, Jerusalem, Israel) was used to verify the output pulse energy from the fiber. The prepared stomach

tissue was fixed by tissue holder and the tip of optical fiber was contacted on the top of mucosal layer in vertical direction. The number of pulse emission was controlled by pulse-counting program in laser system and various number of pulse (#1~30 pulses) were tested on the prepared samples. Each condition was repeated five times ($N = 5$). Due to a physical damage occurred by pulsed laser treatment, the tip of fiber was examined before and after the experiments in order to maintain constant power of laser output.



(a)



(b)

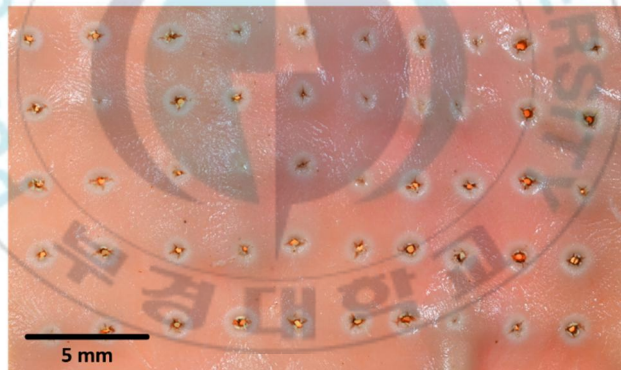


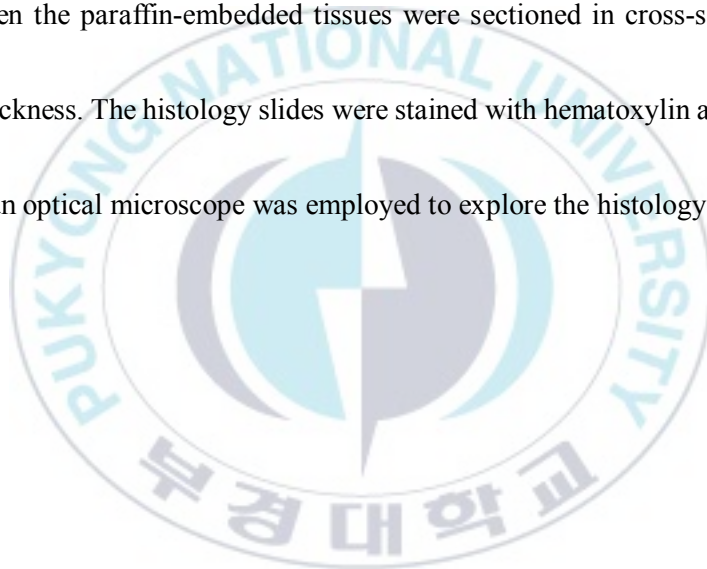
Figure 3. (a) Schematic diagram of experimental set-up for tissue ablation by using optical fiber (M: mucosal layer, SM: submucosal layer, and MP: Muscular propria) and (b) top-view image of laser-treated stomach sample.

2.2.3. Characterization of photothermal responses

After laser treatments on the prepared sample, top images of each laser-treated specimen were taken by employing a digital camera. Then, all samples were stored at $-15\text{ }^{\circ}\text{C}$ for 10 minutes and the frozen samples were cut in 2-mm slices to observe cross-sectional surface of laser ablated groove. After the images were achieved with the camera, Image J (National Institute of the Health, Bethesda, MD) was used to quantify the extent of thermal damage and ablation depth. The depth of tissue ablation was defined as the distance from top of surface to bottom of ablation groove by using Image J (Fig. 4(b)). The extent of thermal damage was measured in five different directions due to irregular occurrence of coagulation. An average value of the five measured distance was employed to characterize thermal damage. Among the #1~#30 laser conditions, #21~#30 were selectively characterized in terms of tissue ablation and thermal damage because only selected groups (#21~#30) showed complete ablation of mucosal layer. The selected 21~30 laser pulses conditions (#21~#30) were compared in graph (Fig. 6) to analyze ablative responses in stomach tissue under various light energy.

2.2.4. Histological analysis

After *ex vivo* experiments, histological study was conducted to observe microscopic variations in the laser-treated stomach tissue. The laser-treated samples were fixed in 10% formalin for 7 days. The fixed tissues were embedded in paraffin block to make histology slides and then the paraffin-embedded tissues were sectioned in cross-sectional surface with 5 μm thickness. The histology slides were stained with hematoxylin and eosin (H&E) method and an optical microscope was employed to explore the histology slides.



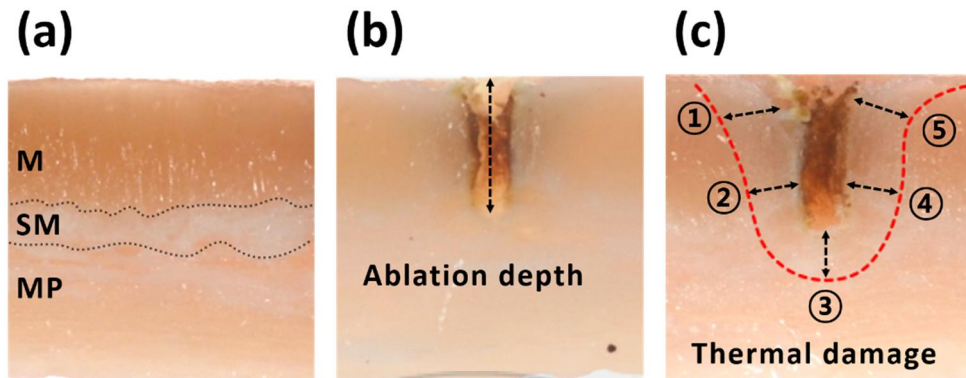


Figure 4. Evaluation of ablation depth and thermal damage in cross-sectional image of laser-ablated stomach tissue: (a) no laser-treated stomach sample (M: mucosal layer, SM: submucosal layer, and MP: muscular propria), (b) definition of ablation depth (a distance from tissue surface to bottom of ablated groove) and (c) thermal damage (an average value of ①~⑤).

2.3. Results

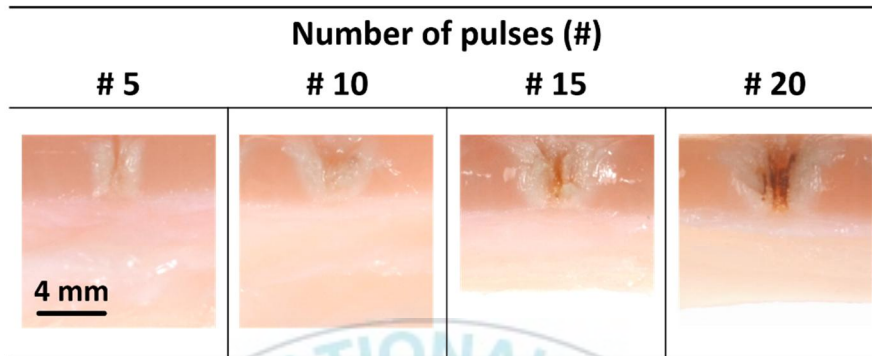
2.3.1. Examination of thermal response in stomach tissue

Figure 5 displays cross-sectional images of Ho:YAG laser-treated stomach tissue under various numbers of pulses conditions. In Fig. 5(a), 5 and 10 pulses of laser irradiation (#5 and #10) mainly induced thermal coagulation in mucosal layer (whitish region) with slight tissue ablation. At the increased number of pulses conditions with #15 and #20, tissue ablation was reinforced and ablation grooves became deeper by augmented light energy. In the cross-sectional image of #20 group, superficial carbonization was presented on ablation groove. However, tissue ablation was confined in mucosal layer by less than 20-J (#20) light energy of Ho:YAG laser. Therefore, higher than 20 times of pulses conditions were selected to complete elimination of mucosal layer. Figure 5(b) compares ablative responses on gastric tissue under #21~#30 conditions. All treatment conditions in Fig. 5(b) remained ablation grooves at focused points with complete elimination of mucosal layer. The ablation depth was increased with increasing number of pulses (# N) and muscular

propria was partially removed by Ho:YAG laser treatment. Although, the ablation grooves became deeper with number of pulses (# N), the thermal damage in surrounding tissue was comparable. All of cases in Fig. 5(b), topical carbonization (black discoloration) was presented on the surface of ablation grooves.



(a)



(b)



Figure 5. Observation of physical deformation in cross-sectional view of laser-treated stomach tissue: (a) comparison of thermal response of stomach tissue by multiple times of laser pulses and (b) ablation grooves in stomach tissue under various number of pulses irradiation (#21~#30).

2.3.2. Evaluation of thermal response in stomach tissue

Figure 6 suggests the normalized ablation depth and thermal damage induced by Ho:YAG laser under #21~#30 treatment conditions. In Fig. 6(a), all of treatment groups in #21~#30 occurred higher than 2 mm of ablation depth, which entirely remove the mucosal layer (~2 mm). The extent of ablation groove was increased with increasing laser pulses. The largest ablation depth (3.3 ± 0.4 mm) occurred at #30 pulses condition, removing a part of muscular propria. The normalized ablation depth at #25 (2.9 ± 0.3 mm) and #29 (2.9 ± 0.3 mm) were 41% and 42% higher than #21 (2.0 ± 0.3 mm) condition. Figure 6(b) shows the normalized thermal damage surrounding ablation grooves in cross-sectional surface of laser-treated stomach tissue. The evaluated thermal damage was the highest at #29 (0.8 ± 0.1 mm) pulses condition. #30 pulses condition yielded 0.8 ± 0.1 mm of thermal damage, which was 18% higher than 0.7 ± 0.1 mm at #21. Unlike the ablation depth, the extent of thermal damage was not augmented by increasing number of laser pulses (#N) and the normalized thermal damage was comparable (0.7~0.8 mm) in all of treatment conditions (#21~#30).

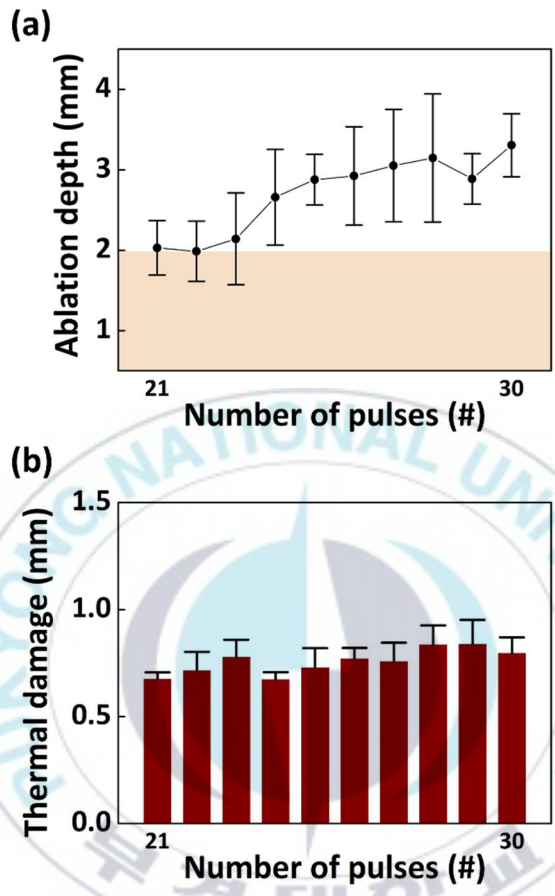
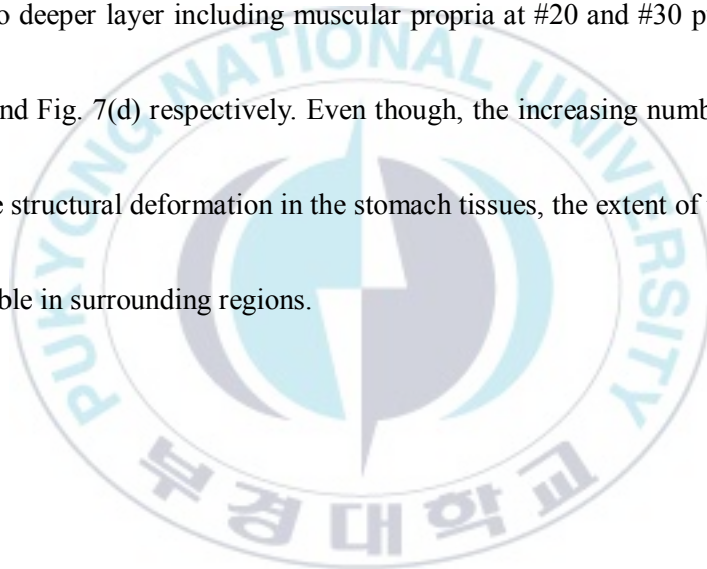


Figure 6. Characterization of thermal response in terms of various number of laser pulses (#21~#30): normalization of (a) ablation depth and (b) thermal damage in laser-treated stomach tissue.

2.3.3. Histological evaluation

Figure 7 suggests histology images of laser-treated lesion in the stomach tissues under #10, #20, and #30 pulses conditions. At #10 pulse condition in Fig. 7(b), narrow ablation groove was generated in part of mucosal layer. However, the amount of tissue ablation was expanded into deeper layer including muscular propria at #20 and #30 pulses conditions in Fig. 7(c) and Fig. 7(d) respectively. Even though, the increasing number of pulses (#) induced more structural deformation in the stomach tissues, the extent of thermal damage was comparable in surrounding regions.



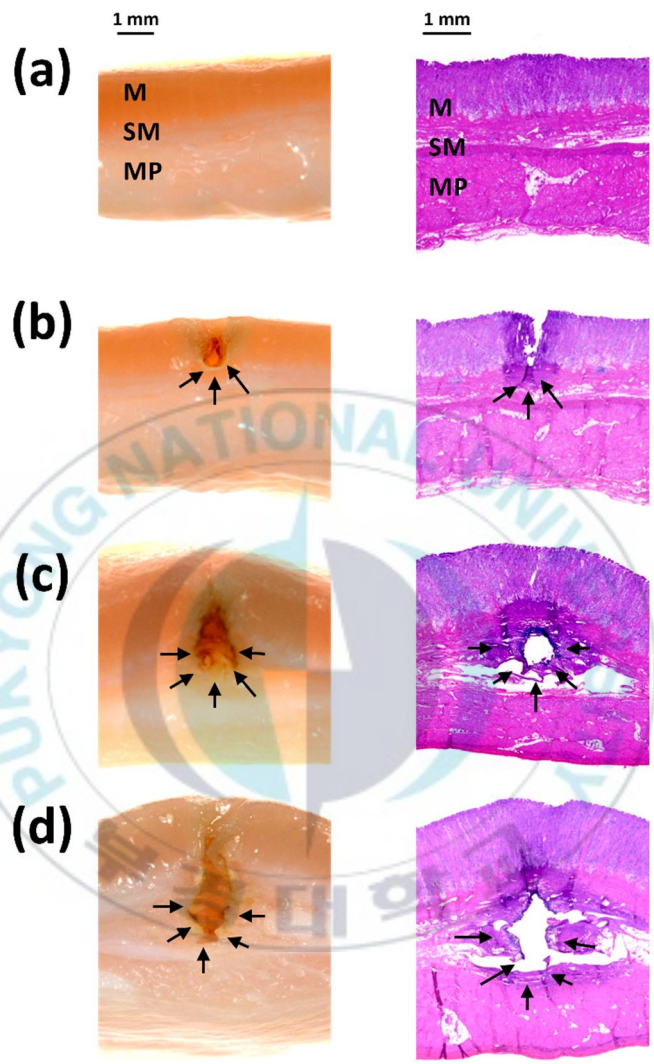


Figure 7. Comparison of laser-ablated stomach tissue in cross-sectional images and histology images under various pulse energies: (a) control, (b) 10 pulses (#10), (c) 20 pulses (#20), and (d) 30 pulses (#30) of Ho:YAG laser irradiations. Black arrows represent ablative regions (M: mucosal layer, SM: submucosal layer, and MP: muscular propria).

3. Translational laser treatment for mucosal incision

3.1. Purpose

The purpose of this study was to evaluate a therapeutic capacity of Ho:YAG laser to implement ESD under various surgical parameters at dynamic condition. It was hypothesized that pulsed Ho:YAG laser can completely incise a mucosal layer with minimized thermal damage to the surrounded tissue. In addition to, occurrence of perforation in the muscular propria by excessive laser treatment can be prevented by saline injection into submucosal layer. A recent study reported clinical results of the Ho:YAG-assisted ESD, however, scientific investigation was not conducted on physical responses of the stomach tissue during laser treatment. Thus, the current study analyzed the photothermal responses of *ex vivo* stomach tissue induced by defined Ho:YAG laser condition in quantitative manner.

3.2. Materials and methods

3.2.1. Experimental set-up for laser treatment

A pulsed Ho:YAG laser system emitted 1 J of pulse energy at 10 Hz (output power = 10 W). A silica optical fiber (core = 375 μm) was coupled to Ho:YAG laser to deliver light energy with established lens system. The lens set-up using both plano-convex lens ($\text{\O} = 12.7$ mm and $f = 20$ mm) and bi-convex lens ($\text{\O} = 25.4$ mm and $f = 50$ mm) were employed to perform non-contact laser-assisted ESD at high radiant exposures. A photodiode sensor was used to monitor output light energy before and after the experiment. The incident light was focused on the tissue surface in a beam diameter of 1 mm. Then, the lens system provided a capacity of the non-contacted light delivery to achieve a high radiant exposure (127 J/cm^2) for tissue ablation. The optical fiber was located vertically 18 mm above the plano-convex lens, and the distance between the plano-convex lens and the bi-convex lens was 80 mm to have constant light collimation. The beam diameter was initially expanded

to 15 mm at the bi-convex lens after the plano-convex lens. Then, the beam was focused on the stomach tissue surface 50 mm below the bi-convex lens.



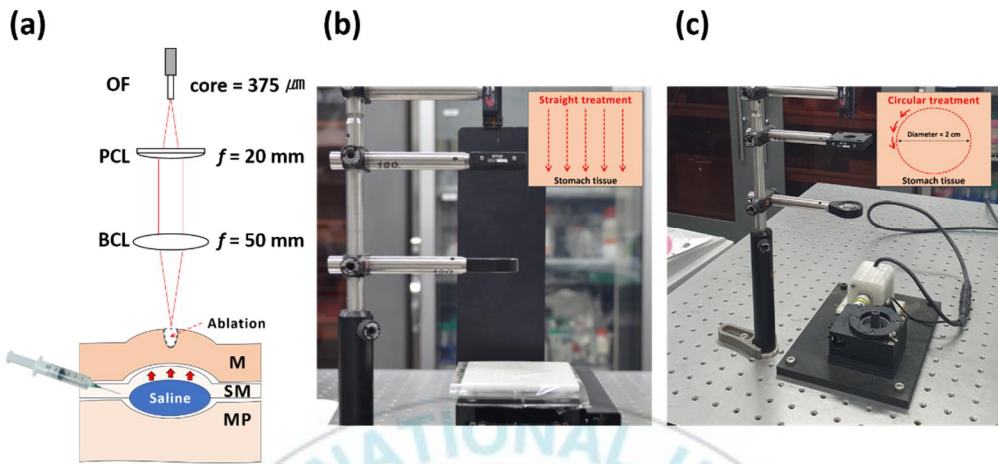


Figure 8. Experimental set-ups for Ho:YAG-assisted ESD on porcine stomach tissue: (a) schematic diagram of lens systems to obtain 1-mm beam diameter on tissue surface, (b) translational stage to attain straight ablation pattern, and (c) rotational stage to achieve circular ablation pattern to emulate clinical ESD (OF: optical fiber, PCL: plano-convex lens, BCL: bi-convex lens, M: mucosal layer, SM: submucosal layer, and MP: muscular propria).

3.2.2. Laser irradiation on no saline-injected stomach tissue

To assess the performance of laser-assisted ESD, various surgical conditions were tested: treatment speed (TS = 0.5, 1, and 2 mm/s) and number of treatment (NT = 1, 2, and 3).

The laser ablation on stomach tissue was performed in a straight pattern to quantify ablation features. Prior to laser treatment, a prepared stomach sample was fixed in tissue holder on a translational stage to reduce any unwanted movement during laser irradiation.

The translational stage was used to create a 2-cm long ablation groove on the tissue surface under defined incision speed. To quantify the amount of increasing incision depth by multiple times of laser irradiation, a straight form of tissue ablation was repeatedly adjusted in same line on the prepared stomach sample. Each laser incision condition was repeated five times (N = 5).

3.2.3. Laser irradiation on saline-injected stomach tissue

To emulate a clinical ESD method, a saline was employed in current *ex vivo* experiment for lifting a mucosal layer from muscular propria. A 10-ml syringe was employed to inject

1-ml saline into four corners of each tissue sample at 2-mm depth, where submucosa was located. After the injection, laser ablation under the same treatment conditions were repeated to identify the effect of the saline injection on the ablative responses of the tissue. Additionally, a circular pattern of laser ablation was also conducted to mimic a clinical ESD procedure. A rotational stage was used to create a circular ablation groove (2 cm in diameter). Once the stage was moved, the Ho:YAG laser was irradiated to ablate the tissue. The circular laser ablation was tested at NT = 3 and TS = 0.5 mm/s without and with saline injection.

3.2.4. Evaluation of laser-ablated stomach tissue

After *ex vivo* experiments, all samples were immediately frozen at - 15 °C and then cut in 1-mm slices. Cross-sectional images of each prepared specimen were taken by using a digital camera to examine ablation depth and the extent of irreversible thermal injury. Image J software was used to measure the ablation depth (i.e., distance from tissue surface to bottom of ablation crater) and the extent of thermal injury (i.e., thickness of thermally

discolored tissue). A total of 40 measurements were taken for each testing condition (N = 40). Student t-test was used for statistical analysis by using SPSS (IBM SPSS Statistics, Chicago, Illinois), and $p < 0.05$ was considered statistically significant.

3.2.5. Histological analysis

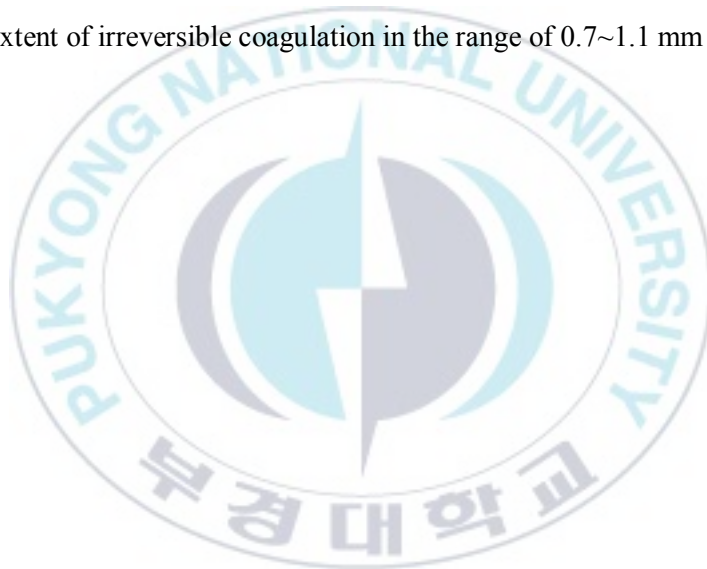
For histological study, the laser-treated samples were fixed in 10 % formalin for 7 days. The tissue-embedded paraffin block was sectioned with 5 μm thickness, which displayed cross-sectional surface of ablation groove. The histology slides were stained with hematoxylin and eosin (H&E) method and an optical microscope was employed to explore the histology slides.

3.3. Results

3.3.1. Evaluation of Ho:YAG-assisted ESD under no saline injection

The ablative responses of stomach tissue without saline injection were compared under various treatment conditions. Figure 9(a) shows the top-view images of the laser-treated tissue. Regardless of treatment speed (TSs), more number of treatments (NTs) accompanied more distinctive carbonization on the ablated grooves. For all NTs, the extent of tissue ablation decreased with increasing TSs. The maximum ablation occurred at NT = 3 and TS = 0.5 mm/s whereas the minimum ablation at NT = 1 and TS = 2 mm/s. For all TSs, the ablated grooves became significantly deeper with NTs in the cross-sectional images of the laser-treated tissues (Fig. 9(b)). An increase in TSs resulted in a shallower ablative groove. NT = 3 and TS = 0.5 mm/s yielded the maximum ablation depth whereas NT = 1 and TS = 2 mm/s showed vivid thermal coagulation (no ablation). Figure 10(a) compares ablation depth as a function of NT and TS. Similarly, the ablation depth increased with increasing NT and decreasing TS. Given NT = 3, the maximum ablation depth was

3.4 ± 0.3 mm (TS = 0.5 mm/s), which was three-fold and two-fold deeper than those at TS = 1 and 2 mm/s, respectively. Thus, NT = 3 and TS = 0.5 mm/s were able to cut the entire mucosal and submucosal layer and a part of muscular propria whereas the rest of the NT and TS conditions partially ablated the mucosal layer. All the NTs and TSs exhibited the comparable extent of irreversible coagulation in the range of 0.7~1.1 mm (Fig. 10(b)).



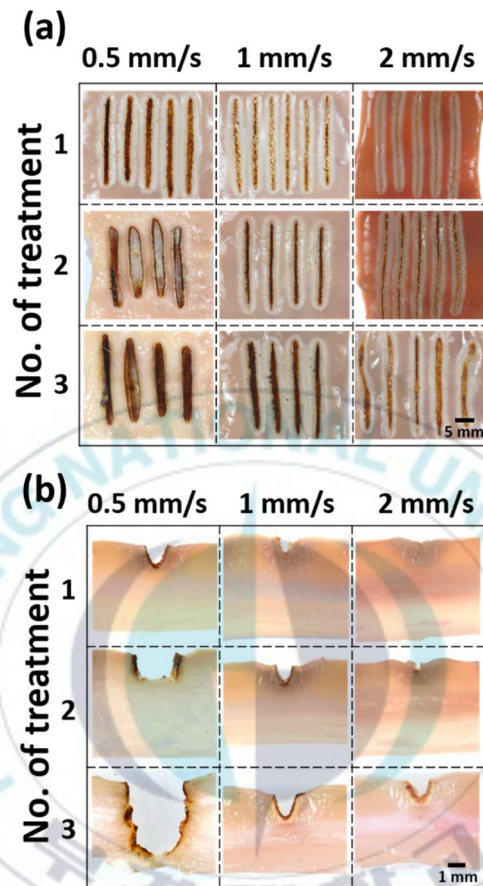
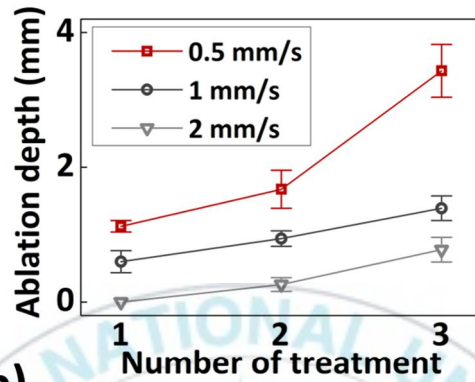


Figure 9. Laser-assisted ESD on ex vivo porcine stomach tissue without saline injection under various surgical parameters: (a) top view images and (b) cross-sectional images of laser-ablated stomach.

(a)



(b)

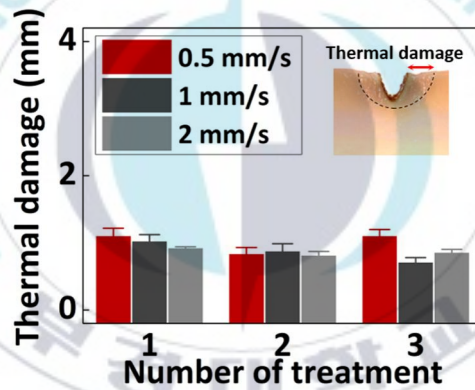


Figure 10. Quantification of thermal response of stomach tissue without saline injection under defined treatment conditions: normalization of (a) ablation depths and (b) extent of irreversible thermal injury.

3.3.2. Evaluation of Ho:YAG-assisted ESD under saline injection

The effect of saline injection in ablative response was investigated under defined treatment conditions. In top-view images, superficial carbonization became evident with increasing NTs (Fig. 11(a)). The extent of tissue ablation increased with increasing NTs and decreasing TSs. The maximum ablation performance was observed at NT = 3 and TS = 0.5 mm/s. Figure 11(b) displays the cross-sectional images of the laser-treated sampled with the saline injection. The ablated areas at TS = 0.5 mm/s became apparently smaller than that without saline injection. Unlike TS = 2 mm/s, TS = 0.5 mm/s showed the distinctive ablation crater at all NTs. The maximum ablation depth was found to be 2.1 ± 0.3 mm at NT = 3 and TS = 0.5 mm/s, which was the only condition to remove the entire mucosal layer and a part of a submucosal layer. Both TSs = 1 and 2 mm/s for all NTs showed that the ablation depth (≤ 1 mm) was thinner than the entire mucosal layer. Thus, NT = 3 and TS = 0.5 mm/s were selected as surgical conditions for circular tissue ablation to emulate clinical ESD. The extent of the irreversible thermal coagulation increased with decreasing TS. The largest thermal injury of 1.1 mm occurred at NT = 3 and TS = 0.5 mm/s. Both

saline conditions demonstrated the comparable extent of irreversible thermal damage in the surrounding tissue (Fig. 10(b) and Fig. 12(b)). The ablation depth and the extent of thermal injury between no saline and saline injections (Table 1 and Table 2). The percent differences between the two cases were calculated by using $(\text{Value}_{\text{saline}} - \text{Value}_{\text{no saline}}) / \text{Value}_{\text{no saline}}$.



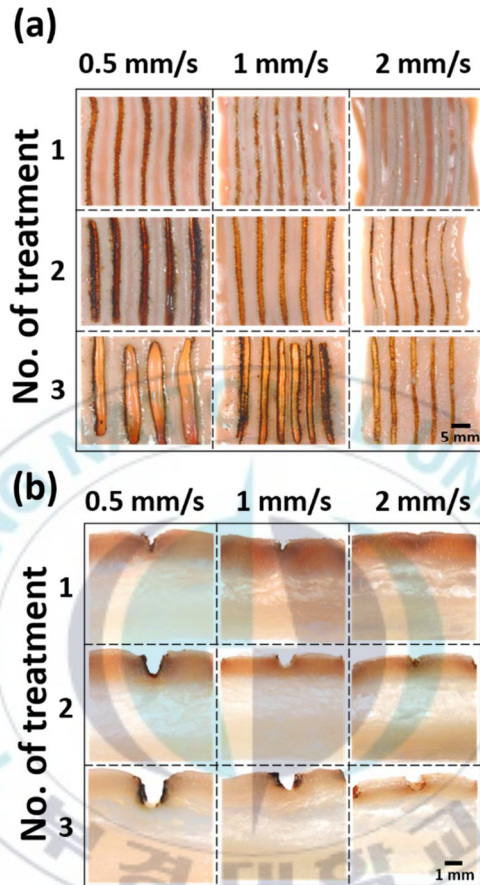
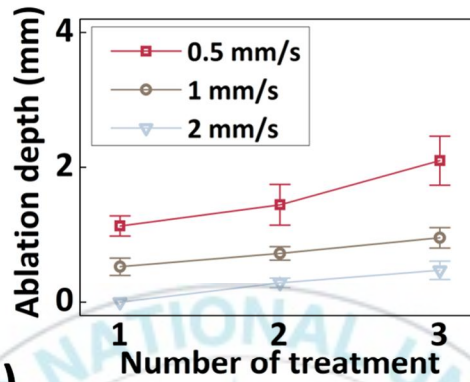


Figure 11. Laser-assisted ESD on ex vivo porcine stomach tissue with saline injection under various surgical parameters: (a) top view images and (b) cross-sectional images of laser-ablated stomach.

(a)



(b)

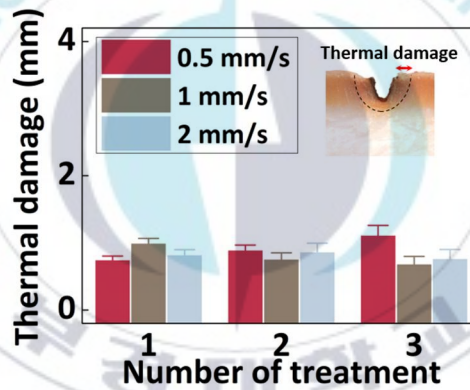


Figure 12. Quantification of thermal response of stomach tissue with saline injection under defined treatment conditions: normalization of (a) ablation depths and (b) extent of irreversible thermal injury.

Table 1. Comparison of ablation depth in tissue between no saline and saline injections

| Treatment speed | Difference (%) [*] | | |
|-----------------|-----------------------------|---------------------|--------------------|
| | Number of treatment | | |
| | 1 | 2 | 3 |
| 0.5 mm/s | 0% (p < 0.05) | -13% (p = 0.663) | -39% (p < 0.05) |
| 1 mm/s | -11% (p = 0.285) | -8% (p < 0.05) | -8% (p = 0.243) |
| 2 mm/s | - | 12% (p < 0.05) | -26% (p < 0.05) |

*percent difference = (depth_{saline} - depth_{no saline}) / depth_{no saline}

Table 2. Comparison of thermal injury in tissue between no saline and saline injections

| Treatment speed | Difference (%) [*] | | |
|-----------------|-----------------------------|---------------------|--------------------|
| | Number of treatment | | |
| | 1 | 2 | 3 |
| 0.5 mm/s | -34% (p = 0.187) | 6% (p = 0.172) | 6% (p = 0.09) |
| 1 mm/s | -3% (p = 0.817) | -14% (p = 0.717) | -4% (p = 0.073) |
| 2 mm/s | -12% (p < 0.05) | 6% (p < 0.05) | -11% (p < 0.05) |

*percent difference = (thermal injury_{saline} - thermal injury_{no saline}) / thermal injury_{no saline}

3.3.3. Characterization of Ho:YAG-assisted ESD in circular pattern

Figure 13(a) shows top-view images of the circularly-ablated tissues with Ho:YAG laser at NT = 3 and TS = 0.5 mm/s without with saline injection. The remaining tissue area ablated without saline injection (top left image) became 23% smaller than the predetermined area (20 mm diameter; area = 314 mm²). The corresponding histology image (top right image) presents that the ablated surface was widely expanded and the ablation depth reached up to muscular propria. On the other hand, the saline-injected tissue ablation (bottom left image) created a relatively larger lesion area with slight shrinkage (~8%) and narrow ablation width. The histology image (bottom right image) confirmed that the narrow tissue ablation reached a submucosal layer, where saline was injected. The thickened submucosal layer (whitish color represents the volumetric tissue dilation due to the saline injection). The ablation depth between no saline and saline injections were compared in Fig. 13(b). Evidently, the no saline injection allowed the incident laser light to ablate the deeper tissue. However, the saline injection case showed that the tissue ablation was stopped in the middle of the submucosal layer with saline injected. It should

be noted that both cases yielded comparable thickness of irreversible thermal injury (~ 1 mm).



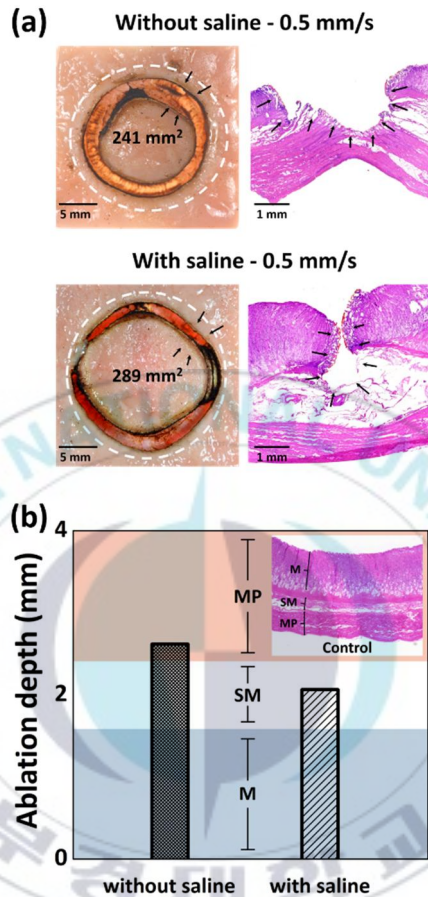


Figure 13. Comparison of circularly-ablated tissue lesion without and with saline injection at NT =3 and TS = 0.5 mm/s: (a) top surface images (left column) and corresponding histology images (right column) and (b) comparison of ablation depth. Black arrows represent the thermally ablated regions (M: mucosal layer, SM: submucosal layer, and MP: muscular propria).

4. Discussion

Endoscopic submucosal dissection is a standardized surgical method to locally remove early gastric cancer from a submucosal layer without damage to the muscle layer underneath. A variety of laser systems have been investigated for laser-assisted ESD to incise the targeted region in a stomach volume without perforation in muscular propria. For instance, cw thulium laser (2 μm) was one of the commercially-available tools used for ESD because of strong light absorption by soft tissue (absorption coefficient = 65 cm^{-1}) [19-22]. However, both long operation time and significant fiber degradation due to tissue contact are still problematic. The cw irradiation typically requires higher laser power (100 W) to effectively ablate tissue, compared to pulsed irradiation [21]. In addition, the thulium-assisted ESD often accompanies excessive smoke that was filled in a hollow organ (e.g., stomach), impeding endoscopic vision and eventually protracting the entire procedure [19, 23]. As another treatment option, cw CO_2 laser (10.6 μm) was also tested for the laser-assisted ESD under ex vivo and in vivo conditions [24-26]. Strong light

absorption by soft tissue contributed to the precise incision of the mucosal layer. The CO₂-assisted ESD took merely 26.2 min of operation time to resect 31.5-mm diameter of ex vivo porcine stomach tissue with submucosal injection. However, the delivery of the far infrared wavelength (10.6 μm) needs to use a hollow waveguide that often associates significant transmission loss due to obstruction of ablated debris at the tip. Thus, compared to both thulium and CO₂ lasers, Ho:YAG laser may provide the potential benefits of having minimal contact tissue ablation at lower average power (10~15 W) and easy use/handling of silica fibers. In fact, the current study presented that the Ho:YAG-assisted ESD took around 10 min to incise a lesion (20 mm in diameter) with insignificant smoke generation. On account of strong light absorption by injected saline, tissue ablation became stopped within the submucosal layer, which can prevent adverse incision perforation in the muscular propria.

The results of static conditions showed that less than 10 J (#10) of Ho:YAG laser occurred shallow tissue ablation with slight coagulation in the mucosal layer and 15 J (#15) was

deficient to perform complete mucosal incision (Fig. 5(a)). To eliminate the entire of mucosal layer, #21~#30 of treatment conditions were tested on the prepared porcine stomach tissue in static environment. Under the controlled pulse energy with 21~30 J (#21~#30) of Ho:YAG laser effectively removed the entire mucosal layer without perforation in muscular propria. It is noticeable that the thermal damage was comparable even under the repeatedly exposure of Ho:YAG laser light rather than expanded into surrounding untargeted tissue. However, it can be problematic that superficial carbonization was generated on the ablation grooves and excessive tissue ablation in the muscular propria by multiple times of laser irradiations (Fig. 5(b)). Thus, more studies will be implemented under various physical conditions of Ho:YAG laser to avoid excessive tissue ablation at static condition.

The translational laser-assisted ESD was performed to adjust a clinical situation incising 2-cm early gastric cancer. In translational conditions, NT =3 and TS = 0.5 mm/s generated the deepest incision under saline injection that could completely ablate the entire mucosa

layer (Fig. 9 and 11). However, other surgical conditions partially incised the mucosal tissue and hardly reached a submucosal layer even under no saline injection possibly because of insufficient energy interactions with tissue. In spite of the complete ablation of the mucosal layer, the surgical conditions of NT =3 and TS = 0.5 mm/s could be laborious and time-consuming under clinical situations. In fact, application of multiple incisions on the same path is quite challenging to perform endoscopically and can result in incomplete incision. In particular, both high pulse energy (1 J) and short pulse durations (200~400 μ s) can generate high pressure (1~2 bar) during ablation due to rapid water vaporization in tissue [27, 28]. The explosive ablation events can apply mechanical impact on the adjacent tissue, leading to expansion of ablated surface (Fig. 11(a)) and possibly to the rupture the surrounding blood vessels and hemorrhage [29]. Thus, compared to the current conditions (1 J at 10 Hz), lower pulse energy (0.3~0.5 J) at higher repetition rates (30~50 Hz) could be more favorable for the Ho:YAG laser to augment a drilling capability for rapidly performing a single incision and to ensure the safety of laser-assisted ESD. In fact, such conditions are clinically available for laser lithotripsy to fragment urinary calculi [30, 31].

Application of multiple pulses with low energy (also known as dusting) can pulverize calculi with ease and simultaneously minimize migration of urinary stone by lowering laser-induced pressure (i.e., mechanical impact). Therefore, further studies will evaluate the Ho:YAG laser with the low pulse energy mode to compare its performance with the current findings and to further explore a therapeutic capacity of the laser-assisted ESD.

Although we investigated the potential application of pulsed Ho:YAG laser for clinical ESD, experimental limitations still remain. The current study merely focused on quantitative characterization of both ablation performance and extent of thermal injury in stomach tissue with saline injected. However, clinical ESD needs to use methylene blue (MB) to lift a submucosal layer and to improve visibility of a target lesion [32, 33]. To complete ESD, the ablated lesion should also be removed from the stomach, which requires a further en bloc resection process in a lateral direction. Furthermore, due to lack of blood perfusion, ex vivo tissue hardly reflects thermal and optical properties of in vivo tissue during ESD. In spite of constant thermal injury of 1 mm, the degree of instant thermal

hemostasis during the laser-assisted ESD should be assessed to warrant the appropriate regulation of potential bleeding. Therefore, further studies should examine the Ho:YAG laser-assisted ESD in in vivo porcine models with MB injection in order to perform the complete ESD process including en bloc resection and to explore acute and chronic responses of the ablated lesion in terms of ESD performance, degree of hemostasis, and wound healing. For the sake of the controlled experimental environments, the current study implemented a lens system in conjunction with a rotational stage to ablate tissue in a noncontact manner. Hence, for clinical translation of the current findings, an optical fiber tip will be designed to have a collimated beam using a micro-lens and evaluated in light of incision performance, degree of invasiveness, and fiber degradation.

5. Summary

The current study investigated the performance of pulsed Ho:YAG laser-assisted ESD on *ex vivo* porcine stomach tissue in both static and dynamic conditions. The results demonstrated that pulsed Ho:YAG laser can be an alternative surgical tool for ESD instead of electrosurgical units. Furthermore, it is noticeable that occurrence of perforation in muscular propria during ESD can be avoided by injected saline below the submucosal layer due to the optical characteristic of 2.1- μm wavelength of laser light. Moreover, further *in vivo* studies will be performed to estimate a clinical feasibility of Ho:YAG-assisted ESD.

6. References

1. Zhu, Z.-L., et al., *Expanding the indication of endoscopic submucosal dissection for undifferentiated early gastric cancer is safe or not?* Asian journal of surgery, 2020. **43**(4): p. 526-531.
2. Facciorusso, A., et al., *Endoscopic submucosal dissection vs endoscopic mucosal resection for early gastric cancer: A meta-analysis.* World journal of gastrointestinal endoscopy, 2014. **6**(11): p. 555.
3. Kakushima, N. and M. Fujishiro, *Endoscopic submucosal dissection for gastrointestinal neoplasms.* World Journal of Gastroenterology: WJG, 2008. **14**(19): p. 2962.
4. Kim, H.J., et al., *Clinical outcomes of early gastric cancer with non-curative resection after pathological evaluation based on the expanded criteria.* PloS one, 2019. **14**(10): p. e0224614.
5. Oka, S., et al., *Advantage of endoscopic submucosal dissection compared with EMR for early gastric cancer.* Gastrointestinal endoscopy, 2006. **64**(6): p. 877-883.
6. Hu, J., et al., *The comparison between endoscopic submucosal dissection and surgery in gastric cancer: a systematic review and meta-analysis.* Gastroenterology Research and Practice, 2018. **2018**.
7. Liu, B., et al., *A novel technique for removing large gastric subepithelial tumors with ESD method in the subcardia region.* Oncology letters, 2019. **18**(5): p. 5277-5282.
8. Oda, I., et al., *Complications of gastric endoscopic submucosal dissection.* Digestive Endoscopy, 2013. **25**: p. 71-78.
9. Kim, E.R. and D.K. Chang, *Management of complications of colorectal submucosal dissection.* Clinical endoscopy, 2019. **52**(2): p. 114.
10. Mahawongkajit, P., *A Single-Center Early Experience of Endoscopic*

- Submucosal Dissection for Gastric Lesions in Thailand*. Gastroenterology Research and Practice, 2020. **2020**.
11. Kim, B.G., et al., *A pilot study of endoscopic submucosal dissection using an endoscopic assistive robot in a porcine stomach model*. Gut and liver, 2019. **13**(4): p. 402.
 12. Larghi, A. and I. Waxman, *State of the art on endoscopic mucosal resection and endoscopic submucosal dissection*. Gastrointestinal endoscopy clinics of North America, 2007. **17**(3): p. 441-469.
 13. Yao, J., et al., *A novel technique using high energy synchronous double-wave laser in endoscopic submucosal dissection of patients with superficial esophageal neoplasm*. Endoscopy, 2018. **50**(12): p. 1175-1179.
 14. Vinnichenko, V., et al. *Comparison of a novel 450-nm laser with Ho: YAG (2100 nm), Tm fiber (1940 nm), and KTP (532 nm) lasers for soft-tissue ablation*. in *Therapeutics and Diagnostics in Urology 2018*. 2018. International Society for Optics and Photonics.
 15. Frenz, M., et al., *Comparison of the effects of absorption coefficient and pulse duration of 2.12-/spl mu/m and 2.79-/spl mu/m radiation on laser ablation of tissue*. IEEE Journal of Quantum Electronics, 1996. **32**(12): p. 2025-2036.
 16. Kamp, S., et al., *Low-power holmium: YAG laser urethrotomy for treatment of urethral strictures: functional outcome and quality of life*. Journal of endourology, 2006. **20**(1): p. 38-41.
 17. Kautzky, M., et al., *Soft tissue effects of the holmium: YAG laser: An ultrastructural study on oral mucosa*. Lasers in Surgery and Medicine: The Official Journal of the American Society for Laser Medicine and Surgery, 1997. **20**(3): p. 265-271.
 18. Mao, Y., et al., *Endoscopic holmium: YAG laser ablation of early gastrointestinal intramucosal cancer*. Lasers in medical science, 2013. **28**(6): p. 1505-1509.
 19. Tontini, G.E., et al., *Ex vivo experimental study on the Thulium laser system:*

- new horizons for interventional endoscopy (with videos)*. Endoscopy international open, 2017. **5**(6): p. E410.
20. Nishioka, N.S. and Y. Domankevitz, *Comparison of tissue ablation with pulsed holmium and thulium lasers*. IEEE journal of quantum electronics, 1990. **26**(12): p. 2271-2275.
 21. Casperon, A.L., et al. *Holmium: YAG ($\lambda=2120\text{nm}$) vs. thulium fiber ($\lambda=1908\text{nm}$) laser for high-power vaporization of canine prostate tissue*. in *Photonic Therapeutics and Diagnostics IV*. 2008. International Society for Optics and Photonics.
 22. Socarrás, M.R., et al., *Thulium: YAG vs Holmium: YAG laser effect on soft tissue: Evidence from an ex vivo experimental study*. European Urology Open Science, 2020. **19**: p. e83-e84.
 23. Cho, J.-H., et al., *Endoscopic submucosal dissection using a thulium laser: preliminary results of a new method for treatment of gastric epithelial neoplasia*. Endoscopy, 2013. **45**(09): p. 725-728.
 24. Morita, Y., et al., *New Development for Safer Endoscopic Submucosal Dissection using the Carbon Dioxide (CO₂) Laser (Secondary publication)*. LASER THERAPY, 2019. **28**(2): p. 89-96.
 25. Obata, D., et al., *Endoscopic submucosal dissection using a carbon dioxide laser with submucosally injected laser absorber solution (porcine model)*. Surgical endoscopy, 2013. **27**(11): p. 4241-4249.
 26. Noguchi, T., et al., *Enhancement of the safety and efficacy of colorectal endoscopic submucosal dissection using a CO₂ laser*. Lasers in Medical Science, 2020. **35**(2): p. 421-427.
 27. Jansen, E.D., et al., *Effect of pulse duration on bubble formation and laser induced pressure waves during holmium laser ablation*. Lasers in Surgery and Medicine: The Official Journal of the American Society for Laser Medicine and Surgery, 1996. **18**(3): p. 278-293.
 28. Chan, K.F., et al., *Holmium: YAG laser lithotripsy: a dominant photothermal*

- ablative mechanism with chemical decomposition of urinary calculi*. Lasers in Surgery and Medicine: The Official Journal of the American Society for Laser Medicine and Surgery, 1999. **25**(1): p. 22-37.
29. Rosen, J., et al., *Biomechanical properties of abdominal organs in vivo and postmortem under compression loads*. Journal of biomechanical engineering, 2008. **130**(2).
 30. Kang, H.W., et al., *Dependence of calculus retropulsion on pulse duration during Ho: YAG laser lithotripsy*. Lasers in Surgery and Medicine: The Official Journal of the American Society for Laser Medicine and Surgery, 2006. **38**(8): p. 762-772.
 31. Lee, H., et al., *Urinary calculus fragmentation during Ho: YAG and Er: YAG lithotripsy*. Lasers in Surgery and Medicine: The Official Journal of the American Society for Laser Medicine and Surgery, 2006. **38**(1): p. 39-51.
 32. Castro, R., et al., *Solutions for submucosal injection: what to choose and how to do it*. World journal of gastroenterology, 2019. **25**(7): p. 777.
 33. Wedi, E., et al., *Endoscopic submucosal dissection with a novel high viscosity injection solution (LiftUp) in an ex vivo model: a prospective randomized study*. Endoscopy international open, 2019. **7**(5): p. E641.

Acknowledgment

석사 과정을 졸업하며 가장 먼저 저를 지도해 주시고 기다려 주신 강현욱 교수님께 제가 표현할 수 있는 최고의 감사를 모아 드립니다. 저의 크고 작은 문제와 진로에 대해 진지하게 고민하여 주시고 제가 삶의 방향을 결정하지 못하고 헤매고 있을 때에 객관적이고 현실적인 시각으로 스스로 냉정한 판단을 내릴 수 있도록 이끌어 주셔서 감사합니다. 연구실 생활동안 교수님께서 가르쳐 주신 귀중한 가치들을 잃어 버리지 않고 기억하며 부지런히 목표를 향해 나아가는 삶을 살기 위해 노력하겠습니다. 이 배움의 시간을 제게 허락해 주신 부모님과 가족에게도 많은 은혜를 입은 것 같습니다. 또한 부족한 저를 이해해 주시고 수많은 조언을 주시며 함께 해 주셨던 연구실분들이 있었음에 대한 감사와 감동은 말로 다 표현할 수 없을 것 같습니다. 제 인생에 다시 있기 어려운 소중한 귀한 인연으로 저를 지원해 주신 모든 분들께 깊이 감사드립니다. 여전히 많이 부족하고 서투른 제 자신이지만 연구실에 있었던 시간들을 인생의 중요한 전환점으로 여기고 어디에 가서든 저가 교수님의 제자임이 부끄럽지 않을 사람이기 위해 노력하겠습니다.

제가 감정의 표현이 드물고 다소 지루한 사람이지만 속으로는 저와 함께 해 주신 여러분께 누구보다 애정이 많고 감사하고 있음을 알아주셨으면 합니다. 다시 한번 제 힘이 되어주신, 은혜로운 시간을 보낼 수 있도록 도와주신 모든 분들께 감사드립니다.